molecular oral microbiology

molecular oral microbiology

Sustained mitogen-activated protein kinase activation with *Aggregatibacter actinomycetemcomitans* causes inflammatory bone loss

J. Dunmyer[1,2], B. Herbert[1], Q. Li[1], R. Zinna[1], K. Martin[1], H. Yu[1] and K.L. Kirkwood[1,2]

1 Department of Craniofacial Biology and the Center for Oral Health Research, Medical University of South Carolina, Charleston, SC, USA
2 Department of Microbiology and Immunology, Medical University of South Carolina, Charleston, SC, USA

Correspondence: Keith L. Kirkwood, Department of Craniofacial Biology, Center for Oral Health Research, Medical University of South Carolina, 173 Ashley Avenue, Charleston, SC 29425, USA Tel.: +8437920969; fax: +8437925312; E-mail: klkirk@musc.edu

Keywords: bone loss; cytokines; host immune response; periodontal disease
Accepted 25 May 2012
DOI: 10.1111/j.2041-1014.2012.00656.x

SUMMARY

Aggregatibacter actinomycetemcomitans **is a gram-negative facultative capnophile involved in pathogenesis of aggressive forms of periodontal disease. In the present study, we interrogated the ability of *A. actinomycetemcomitans* to stimulate innate immune signaling and cytokine production and established that *A. actinomycetemcomitans* causes bone loss in a novel rat calvarial model. *In vitro* studies indicated that *A. actinomycetemcomitans* stimulated considerable production of soluble cytokines, tumor necrosis factor-α, interleukin-6 and interleukin-10 in both primary bone marrow-derived macrophages and NR8383 macrophages. Immunoblot analysis indicated that *A. actinomycetemcomitans* exhibits sustained activation of all major mitogen-activated protein kinase (MAPK) pathways, as well as the negative regulator of MAPK signaling, MAPK phosphatase-1 (MKP-1), for at least 8 h. In a rat calvarial model of inflammatory bone loss, high and low doses of formalin-fixed *A. actinomycetemcomitans* were microinjected into the supraperiosteal calvarial space for 1–2 weeks. Histological staining and micro-computed tomography of rat calvariae revealed a significant increase of inflammatory and fibroblast infiltrate and increased bone resorption as measured by total lacunar pit formation. From these data, we provide new evidence that fixed whole cell *A. actinomycetemcomitans* stimulation elicits a pro-inflammatory host response through sustained MAPK signaling, leading to enhanced bone resorption within the rat calvarial bone.**

INTRODUCTION

Periodontal disease is a chronic inflammatory disease marked by inflammation in gingival tissue and alveolar bone resorption that commonly lead to tooth loss (Page & Schroeder, 1976). In humans, a subgingival biofilm containing *Aggregatibacter actinomycetemcomitans*, a gram-negative capnophile, is associated with aggressive forms of periodontal disease in juveniles and adults (Lopez *et al.*, 1996; Tinoco *et al.*, 1997; Slots & Ting, 1999; Takeuchi *et al.*, 2003; Kamma *et al.*, 2004). In a susceptible host, *A. actinomycetemcomitans* endotoxin stimulates the release of pro-inflammatory mediators such as cytokines and prostaglandins that lead to destruction of periodontal tissues.

Bacterial constituents activate the innate immune response through toll-like receptors (TLRs) and

© 2012 John Wiley & Sons A/S

promote subsequent release of cytokines. *Aggregatibacter actinomycetemcomitans*-derived lipopolysaccharide (LPS), a gram-negative cell wall component, induces the mitogen-activated protein kinase (MAPK) pathway. MAPKs are a family of serine/threonine proteases, and include p38, extracellular signal-related kinases (ERK1/2) and c-Jun N-terminal kinases (JNK). Specifically, MAPK-activated protein kinase 2 (MK2) and MAPK phosphatase-1 (MKP-1) regulate inflammatory bone loss in periodontal disease (Li *et al.*, 2011; Yu *et al.*, 2011a). Moreover, MK2 is targeted and phosphorylated by p38 MAPK. *In vivo*, silencing MK2 attenuates LPS-induced inflammatory bone loss in a rat periodontal disease model (Li *et al.*, 2011). Contrary to MK2, MKP-1 regulates MAPKs by dephosphorylating proteins activated upon TLR signaling. MPK-1 is anti-inflammatory in *A. actinomycetemcomitans* LPS-induced bone loss in a periodontal disease rat model (Yu *et al.*, 2011a).

Stress-induced activation of the MAPK pathway causes downstream regulation of host-derived inflammatory cytokines and prostanoids such as tumor necrosis factor-α (TNF-α), interleukin-6 (IL-6), IL-1β,and prostaglandin E_2 (PGE_2) that directly or indirectly cause subsequent bone loss (Ishimi *et al.*, 1990; Tsai *et al.*, 1995; Chen *et al.*, 1998; Zou & Bar-Shavit, 2002; Rogers *et al.*, 2007). These pro-inflammatory mediators lead to activation of matrix metalloproteinases that destroy the matrix in tissue surrounding the tooth (Rogers *et al.*, 2007).

Inflammation in periodontal disease markedly enhances osteoclastogenesis in the alveolar bone(Hall & Chambers, 1996). Alveolar bone turnover that is normally coupled is indisequilibrium in the periodontal disease state, leading to net bone loss (Rogers *et al.*, 2007). Interestingly, IL-1 and TNF-α can induce osteoclastogenesis directly by nuclear factor-κB ligand (RANKL), a TNF family cytokine, or indirectly through IL-6 (Rogers *et al.*, 2007). Osteoblasts respond to IL-1β, PGE_2 and TNF-α to upregulate RANKL and stimulate osteoclast differentiation (Roux & Orcel, 2000).

To experimentally model the osteoimmunological host response in periodontal disease, small animal models are commonly used. For example, *A. actinomycetemcomitans* inoculation by oral gavage, *A. actinomycetemcomitans* LPS palatal injections, oral *A. actinomycetemcomitans* inoculation, or live *A. actinomycetemcomitans* in feeding, mimic a periodontal disease host inflammatory response in rats or mice (Garlet *et al.*, 2006; Fine *et al.*, 2009; Yu *et al.*, 2011a). Although *A. actinomycetemcomitans* LPS elicits a host response when injected into the palatal maxillae of rats, *A. actinomycetemcomitans* contains other virulence factors associated with aggressive periodontitis, such as cytolethal distending toxin, which can contribute to pathogenesis by inhibiting both cellular and humoral immunity via apoptosis of immune response cells (Tan *et al.*, 2002; Rogers *et al.*, 2007).Therefore, whole *A. actinomycetemcomitas* stimulation is necessary to obtain a more comprehensive appreciation for the bacterially induced host response.

In this study, we address the MAPK host intracellular signaling pathway, through stimulation with formalin-fixed *A. actinomycetemcomitans* in rat macrophages and *in vivo* using a rat calvarial model. The *A. actinomycetemcomitans* expounds the contribution of the host immune response to periopathogenic bacterial stimulation and osteoimmunological impact on bone destruction.

METHODS

Bacterial preparation

Aggregatibacter actinomycetemcomitans Strain Y4 was grown on 5% sheep blood agar plates (Becton Dickinson, Franklin Lakes, NJ) for 36–48 h at 37°C with 10% CO_2 with a large liquid culture prepared in NIH thioglycollate (Becton Dickinson) under the same conditions. Harvested bacteria were centrifuged and fixed in 4% paraformaldehyde for 1 h and then washed extensively with 5% glycerol in phosphate-buffered saline (PBS). A final bacterial suspension in PBS was at a concentration of 4×10^9 cells ml^{-1}. The *A. actinomycetemcomitans* LPS was extracted from strain Y4 by the hot phenol–water method as previously described (Rogers *et al.*, 2007). The LPS used in this study contained <0.001% nucleic acid by spectrophotometry and approximately 0.7% protein by bicinchoninic acid protein assay (Pierce, Rockford, IL) as described previously(Rogers *et al.*, 2007).

Macrophage culture

NR8383 cells (rat macrophage) were purchased from the American Type Culture Collection (ATTC,

© 2012 John Wiley & Sons A/S

Manassas, VA). This rat macrophage cell line was established from normal rat alveolar macrophage cells that were obtained by lung lavage. Cells were maintained in Ham's F-12 medium with 15% fetal bovine serum. Primary bone-marrow-derived macrophages (BMMϕ) were harvested from adult male Sprague-Dawley rats (Harlan Laboratories, Inc., Indianapolis, IN). The femurs and tibias were flushed with α-minimum essential medium (αMEM; Invitrogen Life Technologies, Grand Island, NY). Total bone marrow cultures were incubated in αMEM containing 10% fetal bovine serum, 2 mM glutamine, 100 μl ml^{-1} penicillin and 100 μg ml^{-1} streptomycin overnight. Non-adherent cells after 24 h of culture were plated for macrophage differentiation using Dulbecco's MEM containing 10% fetal bovine serum, 2 mM glutamine, 50 ng ml^{-1} murine macrophage-colony stimulating factor (R&D Systems, Minneapolis, MN), 100 μl ml^{-1} penicillin and 100 μg ml^{-1} streptomycin. BMMϕ were established after 7 days under these conditions as described previously (Yu *et al.*, 2011b).

Immunoblot and enzyme-linked immunobsorbent assay

Activation of the select MAPK/MKP/nuclear factor-κB (NF-κB) signaling pathways was evaluated using total protein extracted from samples harvested at the indicated time points following stimulation with *A. actinomycetemcomitans* LPS (100 ng ml^{-1}). Protein samples were obtained using a commercially available extraction buffer, supplemented with phenylmethylsulphonyl fluoride, protease inhibitors in sodium dodecyl sulfate–polyacrylamide gel electrophoresis buffer (BioRad, Hercules, CA). Total cellular lysate (25 μg) was electrophoresed on 10% denatured sodium dodecyl sulfate–polyacrylamide gel electrophoresis gels and transferred to nitrocellulose membranes (BioRad). Antibodies against phosphorylated and non-phosphorylated forms of p38, JNK, ERK MAPK, MK2, NF-κB and NF-κB p65 (Cell Signaling Technologies, Danvers, MA), along with MKP-1 (Santa Cruz Biotechnology, Inc., Santa Cruz, CA) were used as primary antibodies in these studies. Primary antibodies were detected using horseradish peroxidase-conjugated secondary antibodies and exposure development against radiographic film using the chemiluminescence system (LumiGlo; Cell Signaling). Radiographic images were obtained on a Gel-Doc XR system and densitometric analysis was performed using QUANTITY ONE software (Bio-Rad). Cytokine expression in cell culture supernatants was measured using the enzyme-linked immunobsorbent assay (ELISA) protocol DuoSet ELISA Development Systems to determine IL-6, TNF-α and IL-10 (R&D Systems, Minneaopolis, MN) according to the manufacturer's instructions.

Calvarial model

The Institutional Animal Care and Use Committee at the Medical University of South Carolina approved all the animal protocols. Adult male Sprague-Dawley rats (Harlan Laboratories) weighing ~250–274 g were used for *in vivo* studies. Rats were maintained under specific pathogen-free conditions in pairs with food and tap water *ad libitum*. Animals were routinely weighed once a week to ensure proper growth and nutrition. Following anesthesia with 5% isoflurane, Sprague-Dawley rats were injected once with 100 μl formalin-fixed *A. actinomycetemcomitans* at 1×10^9 and 1×10^8 cells ml^{-1}, *A. actinomycetemcomitans* LPS (250 μg in 25 μl), or PBS control in the mid-sagittal suture area near the supraperiosteal region of the rat calvarium using a 26-gauge needle and a Hamilton syringe. The PBS + vehicle controls consisted of an empty 50-ml tube treated under the same formalin fixation conditions without bacteria.

Micro-computed tomography imaging

Harvested calvarial samples were fixed for 24 h in 10% formalin and then changed to 70% ethanol. Samples were scanned by micro-computed tomography (μCT) (GE Healthcare, Chalfont St Giles, Buckinghamshire, UK). Each scan was reconstructed at a mesh size of 18 μm^3, and three-dimensional digitized images were generated for each sample using GE Healthcare MICROVIEW software (version + 2.0 build 0029). By using μCT analysis it is possible to view the scans from almost any angle or cross-section so as to retrieve an accurate bone volumetric fraction analysis. Therefore, a standardized orientation of the images was necessary before measurement. Region of interest landmarks for resorption pit enumeration were set using the coronal sutures adjacent to the occipital bone; the coronal sutures adjacent to the

© 2012 John Wiley & Sons A/S

nasofrontal area; and the lambdoid sutures creating a four-point connected square from the superior view. All μCT scans were measured and assessed by an independent examiner in a blinded manner.

Histological examination

Formalin-fixed, decalcified maxillae were embedded in paraffin, and serial sagittal sections (7-μm) were prepared. Some slides were stained routinely with haematoxylin & eosin for descriptive histology. Histological images were acquired using an Olympus BX61 Research microscope (Olympus, Center Valley, PA) fitted with a DP71 digital camera. The inflammatory cell infiltrate and fibroblast scores were quantified using a pathological scoring system ranging from 0 to 4. A score of 0 indicated no significant inflammatory infiltrate, 1 was mild (<500), 2 was moderate (500–1000), 3 was severe (1001–1500), and 4 was extremely severe (>1500). A fibroblast score of 0 indicated no proliferation with no fibrotic band, 1 was mild with a thin band, 2 was moderate with a moderately thick band, 3 was severe with a thick band, and 4 was extremely significant fibroblast number with an extremely thick band.

Osteoclast measurement

To quantify osteoclasts, tartrate-resistant acid phosphatase (TRAP) staining was performed in tissue sections using a leukocyte acid phosphatase kit (Sigma Aldrich, St Louis, MO). Mature osteoclasts were counted as TRAP-positive multinucleated (at least three nuclei) in contact with the bone surface. Slides from serial sagittal sections were used to enumerate TRAP-positive cells. The tissue sections were counterstained with haematoxylin after TRAP staining.

Statistical analysis

Pairwise comparisons between experimental groups were performed using the Student's *t*-test with Welch's correction for unequal variances or identified by one-way analysis of variance. *Post-hoc* power analysis confirmed *in vivo* experimental trials. *P*- values <0.05 were considered significant. All calculations were performed using PRISM 4 software (GraphPad, Inc., La Jolla, CA).

RESULTS

Induced cytokine expression after *A. actinomycetemcomitans* stimulation

For these studies we chose to elucidate activated signaling pathways by stimulating (NR8383) rat macrophage cell lines (1×10^6 cells well^{-1}) with formalin-fixed, whole *A. actinomycetemcomitans* bacteria at high and low doses. Cells were harvested after 24 h following microbial stimulation. Expression of candidate targets was tested independently by ELISA using cell culture supernatant. Exposure to the periopathogenic stimulus resulted in significantly increased levels of TNF-α ($P < 0.0001$), IL-6 ($P < 0.0001$) and IL-10 ($P < 0.0001$) in NR8383 cell lines, in comparison with controls (Fig. 1A–C). To verify that these stimulatory effects were not limited to cell lines, primary rat BMMϕ were treated in the same manner. As shown in Fig. 1D–F, TNF-α, IL-6 and IL-10 ($P < 0.0001$) cytokine levels were all significantly elevated after *A. actinomycetemcomitans* exposure.

Activation of MAPK signaling pathway

Production of inflammatory cytokines, including TNF-α and IL-6, are closely related to the activation of the MAPK pathway and NF-κB (Soloviev *et al.*, 2002; Rogers *et al.*, 2007). NR8383 rat macrophage and primary BMMϕ were exposed to 400 colony-forming units (CFU) of formalin-fixed *A. actinomycetemcomitans* or controls and harvested at the indicated timepoints after bacterial exposure. Previously, our group has shown that endotoxin stimulation activates protein kinases including ERK, JNK and p38 MAPK in a manner consistent with formalin-fixed *A. actinomycetemcomitans* stimulation (Li *et al.*, 2011; Yu *et al.*, 2011a). Remarkably, immunoblotting analysis also revealed activation of targeted protein kinases, ERK, JNK and p38 MAPK, as indicated by an increase in phosphorylated expression starting 30 min after stimulation in tissue culture in both a rat macrophage cell line and primary cultured macrophages (Fig. 2). In addition, these studies indicate that MKP-1, a negative regulator of MAPK signaling, and MK2, a downstream substrate of p38 MAPK, has sustained activation for up to 8 h of bacterial exposure (Fig. 2; see Supplementary material, Fig. S1). This unexpected prolonged response was in contrast to the

© 2012 John Wiley & Sons A/S

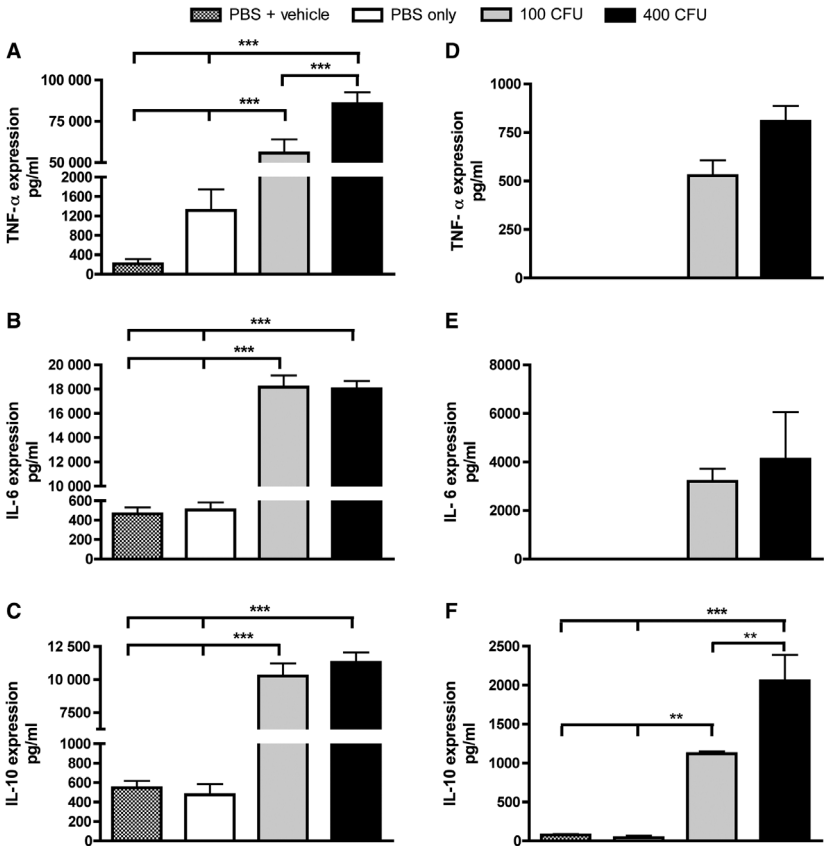

Figure 1 Pronounced expression of inflammatory cytokines was observed in *Aggregatibacter actinomycetemcomitans*-stimulated rat macrophage cells and primary bone marrow-derived macrophages (BMMϕ). NR8383 cells were stimulated with *A. actinomycetemcomitans* for 24 h and cytokine expression was measured by enzyme-linked immunosorbent assay (ELISA) for tumor necrosis factor-α (TNF-α (A), interleukin-6 (IL-6) (B), and IL-10 (C).Following isolation and culturing for 7 days, BMMϕ were stimulated with *A. actinomycetemcomitans* for 24 h and ELISA analysis was used to measure TNF-α (D), IL-6 (E), and IL-10 (F). Representative data of five separate experiments are presented. (**$P < 0.001$, ***$P < 0.0001$).

previous findings where cells displayed a significant increase in protein levels between 60 and 300 min following LPS stimulation, peaking from 30 to 120 min with subsequent downregulation (Li *et al.*, 2011; Yu *et al.*, 2011a). Results using primary macrophages indicate that results are not cell-line specific (Fig. 2B).

Induction of bone resorption

Inflammatory cytokine release can result in bone resorption as a consequence of the elicited host immune response to oral pathogens. In most cases this signaling activity is for protection, but if uncontrolled this may ultimately lead to alveolar bone loss. In the present study, *A. actinomycetemcomitans* with control samples was delivered to the mid-sagittal suture area near the supraperiosteal region of rat calvaria. Animals were sacrificed 1 or 2 weeks after injection and the harvested calvariae and surrounding tissues were initially scanned by μCT to examine changes in calvarial bone resorption within the defined landmarks. Areas of resorption were identified as engraved pits (Fig. 3A). We observed that bacterially stimulated rat calvarial tissues displayed greater lacunar formation in comparison with LPS and vehicle control samples (Fig. 3B). Quantitatively, we found that areas of lacunar resorption dominated areas of the *A. actinomycetemcomitans* (high dosage) micro-delivery within the rat calvariae within specified landmarks of interest, in comparison to controls or LPS at the 2-week harvest (Fig. 3B). The decrease in lacunae from 1 to 2 weeks with the low dosage of *A. actinomycetemcomitans* compared with

© 2012 John Wiley & Sons A/S

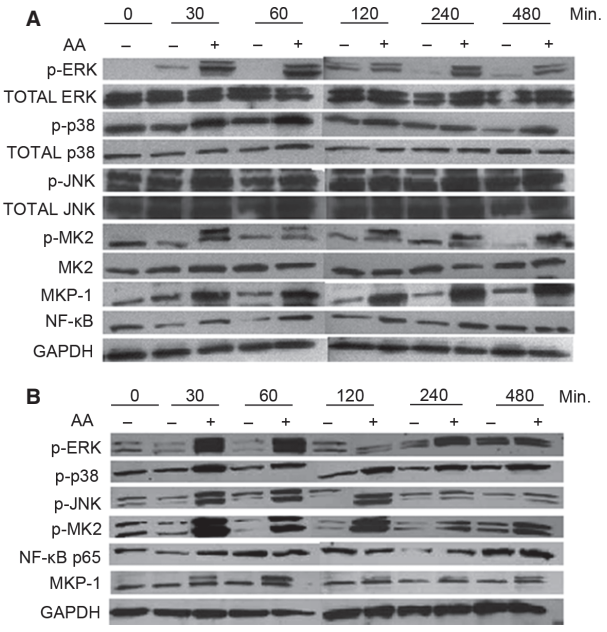

Figure 2 Sustained activation of mitogen-activated protein kinase (MAPK) signaling pathway in rat macrophages and bone marrow-derived macrophages (BMMϕ) following *Aggregatibacter actinomycetemcomitans* stimulation. Sustained activation of intracellular signaling nuclear factor-κB (NF-κB) and MAPK/MAPK phosphatase (MKP) pathways is observed after stimulation with *A. actinomycetemcomitans* in NR8383 rat macrophage cells (A) and BMMϕ (B). Western blot data representative of three separate experiments for (A) and two separate experiments in (B) are shown.

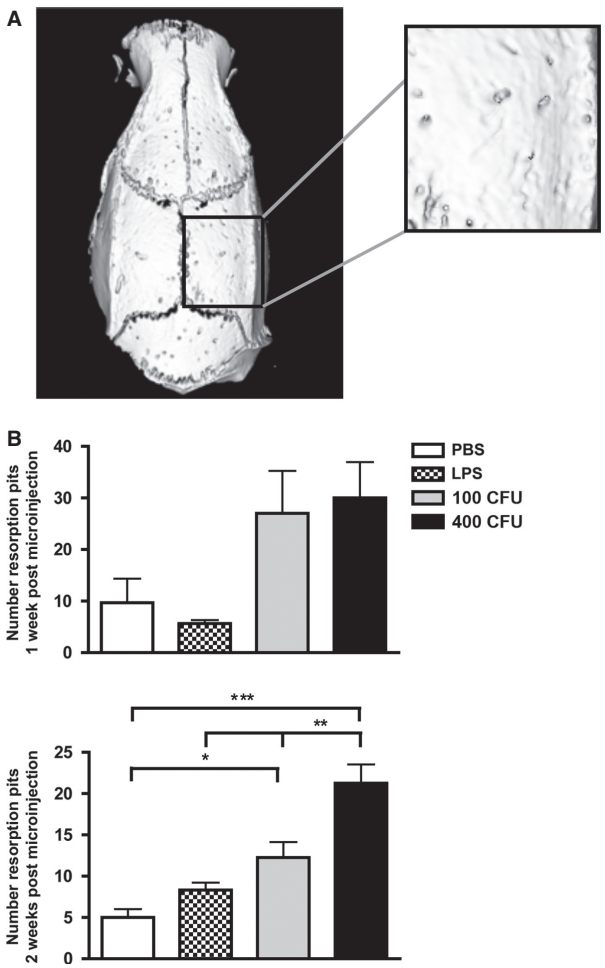

Figure 3 Induction of bone resorption following *Aggregatibacter actinomycetemcomitans* microinjection. Computer rendered micro-computed tomography (μCT) images of representative calvaria samples 2 weeks after exposure to *A. actinomycetemcomitans*. Magnification indicates bone resorption lacunae (A). Enumeration of bone resorption areas at 1 week (upper panel) and 2 weeks (lower panel) after bacterial stimulation (B). Data are expressed as mean number of resorption lacunae ($n = 6$ for controls and $n = 8$ for *A. actinomycetemcomitans* injected samples; $^{***}P < 0.0001$, $^{**}P < 0.001$, $^{*}P < 0.05$).

the high dosage at week 2 suggests that inflammation resolution and bone coupling are occurring. Two weeks post-injection, the 400 CFU dosage of *A. actinomycetemcomitans* was still sufficient to sustain an osteoclastically predominated event to maintain resorption craters compared with a 100 CFU dosage *A. actinomycetemcomitans*.

Inflammatory cell infiltration, fibroblast proliferation and osteoclastogenesis

Rat calvarial tissues were fixed and embedded for histological staining by haematoxylin & eosin. An influx of inflammatory cell infiltrate following *A. actinomycetemcomitans* microinjection was observed in representative sections from the harvested rat calvarie (Fig. 4A). Following blinded pathological enumeration, cell types and tissue environment included robust inflammatory infiltrate numbers within the connective tissues, and numerous capillaries. In contrast, haematoxyin & eosin staining indicated low levels of inflammatory cell infiltrate in control samples (Fig. 4A). The inflammatory score was significantly increased in rats treated with LPS ($P < 0.05$) and 400-CFU dosage *A. actinomycetemcomitans* ($P < 0.05$) 1 week after injection when compared with the PBS (Fig. 4B). Two weeks after injection, the 100-CFU ($P < 0.05$) and 400-CFU ($P < 0.001$) dosages of *A. actinomycetemcomitans* produced a significant increase in inflammatory infiltrate compared to the control. The inflammatory infiltrate in the 400-CFU dosage group

© 2012 John Wiley & Sons A/S

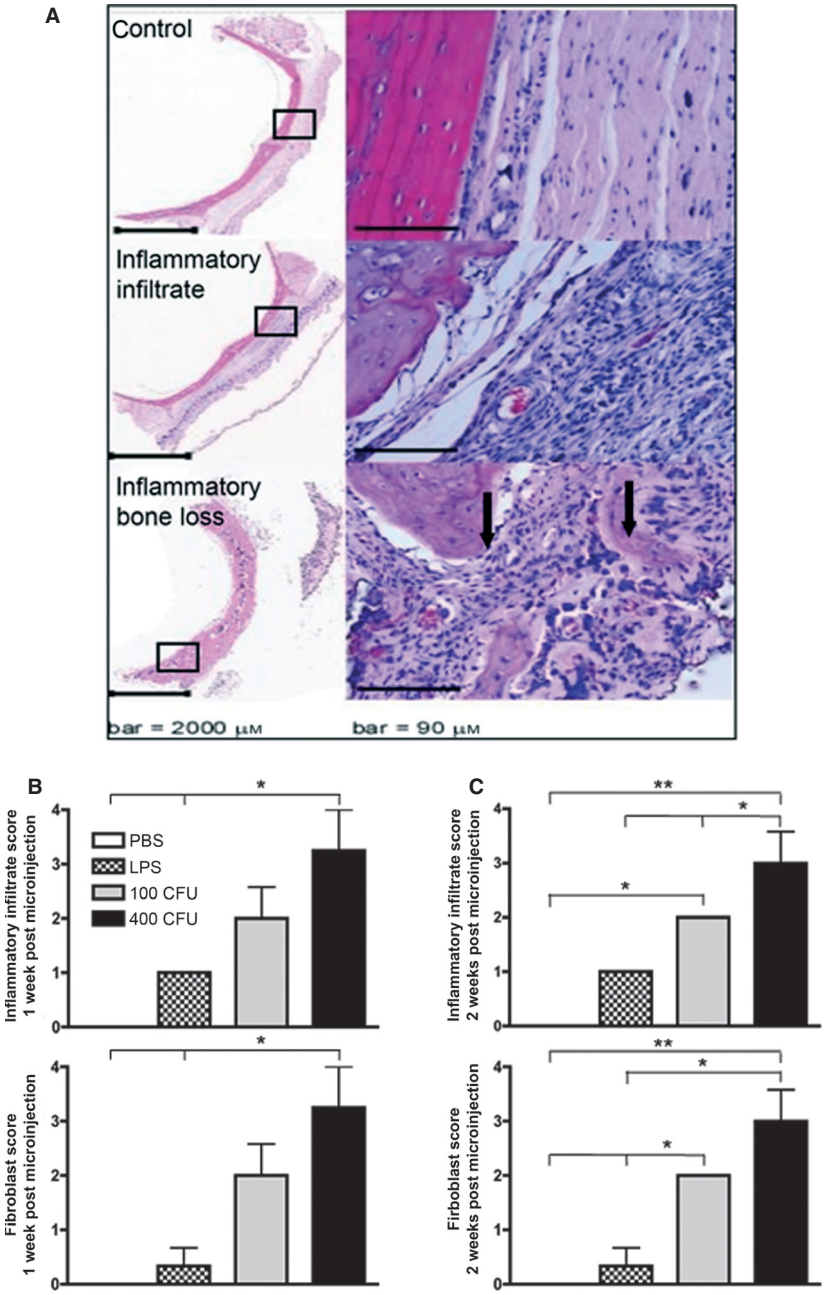

Figure 4 Pronounced inflammatory cell and fibroblast infiltration following *Aggregatibacter actinomycetemcomitans* stimulation. Histological examination of rat calvarial tissues was used to evaluate the extent of inflammatory infiltrate and fibroblast infiltrate. Representative haematoxylin & eosin samples are presented indicating control (phosphate-buffered saline) injected (upper panel), and *A. actinomycetemcomitans*-injected samples (middle and lower panels) showing inflammation and bone resorption respectively. Inflammatory cell infiltrate and fibroblast proliferation were enumerated by a pathological scoring system (B, C). Results are expressed as mean with SE ($n = 6$ for controls and $n = 8$ for *A. actinomycetemcomitans*-injected samples; $^{**}P < 0.001$, $^{*}P < 0.05$).

was also significantly different from LPS ($P < 0.05$) and 100 CFU dosage groups ($P < 0.05$) (Fig. 4C). Upon microinjection, the fibroblast score increased in the 400-CFU dosage group compared with LPS during weeks 1 and 2 ($P < 0.05$) and control groups at week 1 ($P < 0.05$) and week 2 ($P < 0.001$) after stimulation (Fig. 4B,C). By the second week, the 100-CFU treatment of *A. actinomycetemcomitans* also produced an increase in the fibroblast proliferation score compared with the PBS-treated and LPS-treated

© 2012 John Wiley & Sons A/S

groups ($P < 0.05$) (Fig. 2C). Inflammatory and fibroblast scores were dependent on potency of stimulus. Therefore, increased host response and healing were necessary during increased dosages. We also show that LPS and *A. actinomycetemcomitans* have a trend towards increased osteoclast formation (TRAP-positive cells with at least three nuclei) (Fig. 5A).

DISCUSSION

The hallmark of destructive periodontal disease is the overproduction of cytokines and other inflammatory mediators – reviewed in Kirkwood & Rossa (2009). Production of cytokines and inflammatory mediators is usually a tightly controlled process that is initiated by external stimuli that are rapidly transduced through the cytoplasm and into the nucleus. Gene expression initiated within the nucleus is accompanied by a significant component of regulation occurring within the cytosol where signaling mechanisms help to regulate mRNA stability and translation, so amplifying and sustaining expression of immune cytokines. In the present study, *A. actinomycetemcomitans* was able to robustly stimulate pro-inflammatory cytokines (TNF-α and IL-6) as well as the anti-inflammatory cytokine IL-10, which was consistent with previous studies using *A. actinomycetemcomitans*-derived LPS (Patil *et al.*, 2004, 2006; Yu *et al.*, 2011a,b).

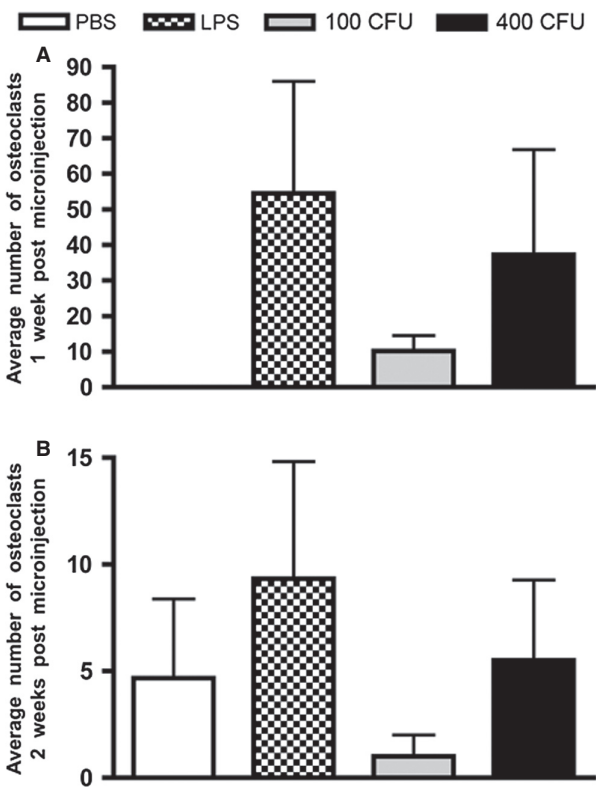

Figure 5 Increased osteoclast formation following lipopolysaccharide (LPS) and *Aggregatibacter actinomycetemcomitans* stimulation. Graphic representation of enumerated tartrate-resistant acid phosphatase-positive ($TRAP^+$) multinucleated formation in calvarial tissue section is presented from indicated groups 1 week (A) or 2 weeks (B) after stimulation. Horizontal bar indicates mean $TRAP^+$ cell counts.

Following TLR engagement, pathogen-associated molecular patterns (PAMPs) stimulate NF-κB and MAPK signaling. Proximal signaling through the p38 MAPK pathway is a well-established cascade essential for inflammatory cytokine expression through regulation of mRNA stability (Patil *et al.*, 2004; Zhao *et al.*, 2011). Attenuation of MAPK signaling occurs through dephosphorylation of activated MAPKs by MKPs, suppressing signaling and MAPK-dependent cytokine expression. Recently, loss-of-function and gain-of-function studies have indicated that MKP-1 is a major signaling protein in *A. actinomycetemcomitans* LPS-induced alveolar loss (Sartori *et al.*, 2009; Yu *et al.*, 2011a). As part of these studies, a kinetic analysis indicated that LPS-activated p38 occurs as early as 10 min but was quickly attenuated at the same time when MKP-1 expression was increased (Sartori *et al.*, 2009). Results from the present study using whole *A. actinomycetemcomitans* indicate a different scenario. In contrast to the reciprocal regulation previously observed, data herein suggest that whole *A. actinomycetemcomitans* stimulates NF-κB and multiple MAPKs including p38, JNK and ERK along with MK2, an immediate downstream kinase substrate of p38, with sustained MAPK activation for up to 8 h in both NR8383 cell lines and primary BMMϕ populations. We speculate that this sustained MAPK activation may be the result of continued TLR activation with multiple PAMPs over time in culture, but additional experiments addressing TLR proximal activation and internalization are needed to substantiate these observations.

In addition to the sustained MAPK activation, we also observed that NF-κB is activated over the same time-frame after whole *A. actinomycetemcomitans* exposure. The TLR signaling requires a different set of adaptors, including myeloid differentiation factor 88 (MyD88) and Toll-IL-1 receptor (TIR) domain-contain-

© 2012 John Wiley & Sons A/S

ing adaptor protein (TIRAP), which will recruit IL-1 receptor-associated kinase 1 (IRAK) or TRAF6. It is currently believed that the kinase transforming growth factor-β-activated kinase 1 (TAK1) would link TRAF6 to the IKK complex, which is a critical regulator for the activation of NF-κB (Hayden & Ghosh, 2004; Tergaonkar, 2006; Garcia de Aquino *et al.*, 2009). Hence, we suspect that activation of the NF-κB canonical pathway occurs after *A. actinomycetemcomitans* exposure in macrophage populations.

A limitation of LPS-induced models of experimental periodontitis is that significant bone loss occurs in mice and rats only after multiple LPS injections (Patil *et al.*, 2006; Rossa *et al.*, 2006; Rogers *et al.*, 2007; Li *et al.*, 2011). In addition, some reports indicate difficulty in rodent colonization with human pathogens, including *A. actinomycetemcomitans* (Schreiner *et al.*, 2011). Although some investigators have been successful using the oral gavage approach (Garlet *et al.*, 2005, 2006, 2008; Gelani *et al.*, 2009; Lima *et al.*, 2010) success may vary depending on specific strains in rat models (Graves *et al.*, 2008; Schreiner *et al.*, 2011). Previous studies inducing periodontal disease require a combination of repeated oral inoculation and palatal injection of *A. actinomycetemcomitans* to elicit a host immune response and bone loss in mice (Garlet *et al.*, 2005).

Hence, in the present study, formalin-fixed *A. actinomycetemcomitans* was used short-term following a single exposure of the periodontal pathogen to address host–bacteria interactions vs. *A. actinomycetemcomitans* virulence. An innate immune response was observed in this model because the rats were naive to the *A. actinomycetemcomitans* before inoculation, making it less likely for an adaptive immune response to occur within the duration of the experiment (Graves *et al.*, 2001). We noticed a sustained inflammatory infiltrate for up to 2 weeks, which is inconsistent with previous findings using *Porphyromonas gingivalis* calvarial injections, which allowed for inflammation to decrease starting at day 5 post-injection (Liu *et al.*, 2004). In addition, our model uses Sprague-Dawley rats with *A. actinomycetemcomitans*. Sprague-Dawley rats are highly susceptible to repeated inoculation of *A. actinomycetemcomitans* LPS, which caused inflammatory bone loss in a periodontal disease model (Rogers *et al.*, 2007). However, it is also possible that we missed peak inflammation at an earlier time-point and that the infiltrate seen at 1 and 2 weeks in our study is resolving. Therefore, it is possible that in this model rats have a diminished ability to resolve inflammation and continue to have sustained infiltrate 2 weeks after injection.

Following 1–2 weeks, we observed an increased number of resorption lacunae in rat calvariae after microinjection of *A. actinomycetemcomitans* in comparison to controls via μCT and TRAP staining for osteoclast formation. It is worth noting that TRAP staining only indicated a trend towards increased osteoclast number that was decreasing in week 2. This may be the result of the osteoclasts undergoing apoptosis at the 2-week time frame and so may not be detectable at this time-point (Tanaka *et al.*, 2006).

This *in vivo* study has identified the consequences of whole bacterial stimulation in rat calvariae in the context of innate immune response. Previously, *A. actinomycetemcomitans* LPS was found to stimulate RANKL, IL-6 and matrix metalloproteinase-13 expression in several periodontal relevant cell types, including periodontal ligament fibroblasts, osteoblasts and macrophages through transcriptional and post-transcriptional mechanisms (Rossa *et al.*, 2005, 2006; Patil *et al.*, 2006). Since the calvarial bone is formed via intramembranous ossification, similar to alveolar bone, this is a suitable model to study the short-term consequences of *A. actinomycetemcomitans* in the host immune interactions as a surrogate for periodontal disease models similar to other studies (Assuma *et al.*, 1998). In summary, we observed sustained MAPK activation and bone resorption in response to activated signaling pathways relevant to cytokine-driven inflammation and bone loss in response to *A. actinomycetemcomitans* stimulation.

ACKNOWLEDGEMENTS

This work was conceived by KLK, laboratory and animal procedures were performed by JD, QL, HY and BH. The manuscript was initially written by JD and revised by KLK and BH. The authors would like to acknowledge the support of Jaclynn Krieder from the Orthopedics Research Core at the University of Michigan. This work was supported by grants from the National Institutes of Health: 1R01DE018290 (KLK), 1R01DE021423 (KLK), 2P20 RR017696 (KLK), and T32 DE017551(BH).

© 2012 John Wiley & Sons A/S

REFERENCES

Assuma, R., Oates, T., Cochran, D., Amar, S. and Graves, D.T. (1998) IL-1 and TNF antagonists inhibit the inflammatory response and bone loss in experimental periodontitis. *J Immunol* **160**: 403–409.

Chen, C.C., Chang, K.L., Huang, J.F., Huang, J.S. and Tsai, C.C. (1998) [Interleukin-6 production by human gingival fibroblasts following stimulation with *Actinobacillus actinomycetemcomitans*]. *Kaohsiung J Med Sci* **14**: 367–378.

Fine, D.H., Schreiner, H., Nasri-Heir, C. *et al.* (2009) An improved cost-effective, reproducible method for evaluation of bone loss in a rodent model. *J Clin Periodontol* **36**: 106–113.

Garcia de Aquino, S., Manzolli Leite, F.R., Stach-Machado, D.R., Francisco da Silva, J.A., Spolidorio, L.C. and Rossa, C. Jr (2009) Signaling pathways associated with the expression of inflammatory mediators activated during the course of two models of experimental periodontitis. *Life Sci* **84**: 745–754.

Garlet, G.P., Avila-Campos, M.J., Milanezi, C.M., Ferreira, B.R. and Silva, J.S. (2005) *Actinobacillus actinomycetemcomitans*-induced periodontal disease in mice: patterns of cytokine, chemokine, and chemokine receptor expression and leukocyte migration. *Microbes Infect* **7**: 738–747.

Garlet, G.P., Cardoso, C.R., Silva, T.A. *et al.* (2006) Cytokine pattern determines the progression of experimental periodontal disease induced by *Actinobacillus actinomycetemcomitans* through the modulation of MMPs, RANKL, and their physiological inhibitors. *Oral Microbiol Immunol* **21**: 12–20.

Garlet, G.P., Cardoso, C.R., Campanelli, A.P. *et al.* (2008) The essential role of IFN-gamma in the control of lethal *Aggregatibacter actinomycetemcomitans* infection in mice. *Microbes Infect* **10**: 489–496.

Gelani, V., Fernandes, A.P., Gasparoto, T.H. *et al.* (2009) The role of toll-like receptor 2 in the recognition of *Aggregatibacter actinomycetemcomitans*. *J Periodontol* **80**: 2010–2019.

Graves, D.T., Oskoui, M., Volejnikova, S. *et al.* (2001) Tumor necrosis factor modulates fibroblast apoptosis, PMN recruitment, and osteoclast formation in response to *P. gingivalis* infection. *J Dent Res* **80**: 1875–1879.

Graves, D.T., Fine, D., Teng, Y.T., Van Dyke, T.E. and Hajishengallis, G. (2008) The use of rodent models to investigate host–bacteria interactions related to periodontal diseases. *J Clin Periodontol* **35**: 89–105.

Hall, T.J. and Chambers, T.J. (1996) Molecular aspects of osteoclast function. *Inflamm Res* **45**: 1–9.

Hayden, M.S. and Ghosh, S. (2004) Signaling to NF-kappaB. *Genes Dev* **18**: 2195–2224.

Ishimi, Y., Miyaura, C., Jin, C.H. *et al.* (1990) IL-6 is produced by osteoblasts and induces bone resorption. *J Immunol* **145**: 3297–3303.

Kamma, J.J., Nakou, M., Gmur, R. and Baehni, P.C. (2004) Microbiological profile of early onset/aggressive periodontitis patients. *Oral Microbiol Immunol* **19**: 314–321.

Kirkwood, K.L. and Rossa, C. Jr (2009) The potential of p38 MAPK inhibitors to modulate periodontal infections. *Curr Drug Metab* **10**: 55–67.

Li, Q., Yu, H., Zinna, R. *et al.* (2011) Silencing mitogen-activated protein kinase-activated protein kinase-2 arrests inflammatory bone loss. *J Pharmacol Exp Ther* **336**: 633–642.

Lima, H.R., Gelani, V., Fernandes, A.P. *et al.* (2010) The essential role of toll like receptor-4 in the control of *Aggregatibacter actinomycetemcomitans* infection in mice. *J Clin Periodontol* **37**: 248–254.

Liu, R., Desta, T., He, H. and Graves, D.T. (2004) Diabetes alters the response to bacteria by enhancing fibroblast apoptosis. *Endocrinology* **145**: 2997–3003.

Lopez, N.J., Mellado, J.C. and Leighton, G.X. (1996) Occurrence of *Actinobacillus actinomycetemcomitans*, *Porphyromonas gingivalis* and *Prevotella intermedia* in juvenile periodontitis. *J Clin Periodontol* **23**: 101–105.

Page, R.C. and Schroeder, H.E. (1976) Pathogenesis of inflammatory periodontal disease. A summary of current work. *Lab Invest* **34**: 235–249.

Patil, C., Zhu, X., Rossa, C. Jr, Kim, Y.J. and Kirkwood, K.L. (2004) p38 MAPK regulates IL-1beta induced IL-6 expression through mRNA stability in osteoblasts. *Immunol Invest* **33**: 213–233.

Patil, C., Rossa, C. Jr and Kirkwood, K.L. (2006) *Actinobacillus actinomycetemcomitans* lipopolysaccharide induces interleukin-6 expression through multiple mitogen-activated protein kinase pathways in periodontal ligament fibroblasts. *Oral Microbiol Immunol* **21**: 392–398.

Rogers, J.E., Li, F., Coatney, D.D. *et al.* (2007) *Actinobacillus actinomycetemcomitans* lipopolysaccharide-mediated experimental bone loss model for aggressive periodontitis. *J Periodontol* **78**: 550–558.

Rossa, C. Jr, Liu, M., Patil, C. and Kirkwood, K.L. (2005) MKK3/6-p38 MAPK negatively regulates murine MMP-13 gene expression induced by IL-1beta and TNF-alpha in immortalized periodontal ligament fibroblasts. *Matrix Biol* **24**: 478–488.

Rossa, C., Ehmann, K., Liu, M., Patil, C. and Kirkwood, K.L. (2006) MKK3/6-p38 MAPK signaling is required for

© 2012 John Wiley & Sons A/S

IL-1beta and TNF-alpha-induced RANKL expression in bone marrow stromal cells. *J Interferon Cytokine Res* **26**: 719–729.

Roux, S. and Orcel, P. (2000) Bone loss. Factors that regulate osteoclast differentiation: an update. *Arthritis Res* **2**: 451–456.

Sartori, R., Li, F. and Kirkwood, K.L. (2009) MAP kinase phosphatase-1 protects against inflammatory bone loss. *J Dent Res* **88**: 1125–1130.

Schreiner, H., Markowitz, K., Miryalkar, M., Moore, D., Diehl, S. and Fine, D.H. (2011) *Aggregatibacter actinomycetemcomitans*-induced bone loss and antibody response in three rat strains. *J Periodontol* **82**: 142–150.

Slots, J. and Ting, M. (1999) *Actinobacillus actinomycetemcomitans* and *Porphyromonas gingivalis* in human periodontal disease: occurrence and treatment. *Periodontol 2000* **20**: 82–121.

Soloviev, A., Schwarz, E.M., Kuprash, D.V. *et al.* (2002) The role of p105 protein in NFkappaB activation in ANA-1 murine macrophages following stimulation with titanium particles. *J Orthop Res* **20**: 714–722.

Takeuchi, Y., Umeda, M., Ishizuka, M., Huang, Y. and Ishikawa, I. (2003) Prevalence of periodontopathic bacteria in aggressive periodontitis patients in a Japanese population. *J Periodontol* **74**: 1460–1469.

Tan, K.S., Song, K.P. and Ong, G. (2002) Cytolethal distending toxin of *Actinobacillus actinomycetemcomitans.* Occurrence and association with periodontal disease. *J Periodontal Res* **37**: 268–272.

Tanaka, S., Miyazaki, T., Fukuda, A. *et al.* (2006) Molecular mechanism of the life and death of the osteoclast. *Ann N Y Acad Sci* **1068**: 180–186.

Tergaonkar, V. (2006) NFkappaB pathway: a good signaling paradigm and therapeutic target. *Int J Biochem Cell Biol* **38**: 1647–1653.

Tinoco, E.M., Beldi, M.I., Loureiro, C.A. *et al.* (1997) Localized juvenile periodontitis and *Actinobacillus actinomycetemcomitans* in a Brazilian population. *Eur J Oral Sci* **105**: 9–14.

Tsai, C.C., Ho, Y.P. and Chen, C.C. (1995) Levels of interleukin-1 beta and interleukin-8 in gingival crevicular fluids in adult periodontitis. *J Periodontol* **66**: 852–859.

Yu, H., Li, Q., Herbert, B. *et al.* (2011a) Anti-inflammatory effect of MAPK phosphatase-1 local gene transfer in inflammatory bone loss. *Gene Ther* **18**: 344–353.

Yu, H., Sun, Y., Haycraft, C., Palanisamy, V. and Kirkwood, K.L. (2011b) MKP-1 regulates cytokine mRNA stability through selectively modulation subcellular translocation of AUF1. *Cytokine* **56**: 245–255.

Zhao, W., Liu, M., D'Silva, N.J. and Kirkwood, K.L. (2011) Tristetraprolin regulates interleukin-6 expression through p38 MAPK-dependent affinity changes with mRNA 3′ untranslated region. *J Interferon Cytokine Res* **31**: 629–637.

Zou, W. and Bar-Shavit, Z. (2002) Dual modulation of osteoclast differentiation by lipopolysaccharide. *J Bone Miner Res* **17**: 1211–1218.

SUPPORTING INFORMATION

Additional supporting information may be found in the online version of this article:

Figure S1. Sustained activation of mitogen-activated protein kinase (MAPK) signaling pathway in rat bone-marrow-derived macrophages (BMMϕ) following *Aggregatibacter actinomycetemcomitans* stimulation. Relative fold change to unstimulated BMMϕ at 0 h was quantified for p-ERK (A), p-p38 (B), p-JNK (C), p-MK2 (D), NF-κB (E) and MKP-1 (F). Graphic representation of densitometry for two independent experiments of immunoblot data was normalized to GAPDH.

Please note: Wiley-Blackwell are not responsible for the content or functionality of any supporting materials supplied by the authors. Any queries (other than missing material) should be directed to the corresponding author for the article.

© 2012 John Wiley & Sons A/S

Copyright of Molecular Oral Microbiology is the property of Wiley-Blackwell and its content may not be copied or emailed to multiple sites or posted to a listserv without the copyright holder's express written permission. However, users may print, download, or email articles for individual use.